JOURNAL OF GEOPHYSICAL RESEARCH, VOL. 112, B06305, doi:10.1029/2006JB004827, 2007

Western Quebec seismic zone (Canada): Clustered, midcrustal seismicity along a Mesozoic hot spot track

Shutian Ma[1] and David W. Eaton[1]

Received 30 October 2006; revised 2 February 2007; accepted 13 February 2007; published 13 June 2007.

[1] The western Quebec seismic zone (WQSZ) is a 160-km-wide band of intraplate seismicity extending 500 km from the Adirondack Highlands (United States) to the Laurentian uplands (Canada). Previous authors have proposed that the WQSZ is localized over the Mesozoic track of the Great Meteor hot spot. Here we explore this hypothesis further by investigating regional seismicity characteristics. Focal mechanisms for WQSZ earthquakes, including a new mechanism for a moderate (mN 4.5) earthquake, reveal a pattern of reverse-sense faulting with SW trending *P* axes changing to E-W in the southern part of the zone. We introduce a simple box-counting method to delineate spatial clusters, based on exceedance of random seismicity density. Combining this approach with focal depths from regional depth phase analysis, we find that seismicity with shallow focus (0–7 km) is characterized by a random spatial distribution, whereas earthquakes with an intermediate focal depth (8–18 km) are strongly clustered along a diffuse linear band trending N50°W. Earthquakes deeper than 18 km are confined to a few distinct clusters. These clusters are characterized by differing *b* values and, for at least one cluster, repeating events. Projection of hypocenters onto a deep seismic profile and comparison with preexisting crustal structures suggest that local reactivation of Precambrian structural features may have occurred; however, the Great Meteor hot spot track remains the only compelling explanation for the overall distribution of earthquakes. Proximity of seismicity clusters to historic and prehistoric earthquakes lends support to the hypothesis that modern seismicity may represent exceptionally long-lived aftershocks of large past events.

Citation: Ma, S., and D. W. Eaton (2007), Western Quebec seismic zone (Canada): Clustered, midcrustal seismicity along a Mesozoic hot spot track, *J. Geophys. Res.*, *112*, B06305, doi:10.1029/2006JB004827.

1. Introduction

[2] The western Quebec seismic zone (WQSZ), as originally defined by *Basham et al.* [1979], is a northwest trending band of seismicity that extends more than 500 km from the Adirondack Highlands of upstate New York (43.5°N, 73.5°W) to the Timiskaming region of Québec, Canada (47.5°N, 79°W; Figure 1). In aggregate, the WQSZ is ~160 km wide, although narrower (50–60 km) subzones have also been recognized [*Forsyth*, 1981; *Adams and Bashan*, 1991; *Lamontagne et al.*, 1994]. Earthquakes of magnitude $M_W \geq 4.5$ occur within the WQSZ several times per decade, most recently including the 2000 Kipawa earthquake [*Bent et al.*, 2002] and the 2002 Au Sable Forks earthquake [*Pierre and Lamontagne*, 2004]. The largest historical event in the WQSZ is the $M = 6.2$ Timiskaming earthquake of 1935 [*Doig*, 1991], while the 1944 Cornwall-Massena earthquake ($M_W = 5.6$) also produced some damage [*Bent*, 1996a]. Recent studies suggest that larger ($M \sim 7$) earthquakes in the WQSZ may have occurred 4550 and 7060 years B.P. [*Aylsworth et al.*, 2000].

[3] Because of its proximity to major population centers, earthquakes in the WQSZ represent the dominant contribution to seismic hazard in the southeastern Canadian cities of Ottawa and Montreal [*Adams and Halchuk*, 2003]. Hazard studies in this region are hindered, however, by lack of a robust model linking earthquakes in the WQSZ to specific seismogenic structures. Although the WQSZ lies almost entirely within the Grenville Province of the Canadian Shield, the relationship of earthquake activity to preexisting structures is not well understood [*Lamontagne et al.*, 1994]. Previous workers have suggested that events within a narrow band of seismicity along the southwestern margin of the WQSZ, including all of the larger historical earthquakes, represent reverse-sense reactivation of Early Paleozoic normal faults within a failed Iapetan rift arm (the Ottawa-Bonnechere Graben [*Forsyth*, 1981; *Bent et al.*, 2002; *Adams and Basham*, 1991]). However, more numerous earthquakes in the northeastern part of the WQSZ lack any consistent spatial relationship with the surface expressions of either rift-related faults or older Grenvillian shear zones [*Forsyth*, 1981; *Adams and Basham*, 1989, 1991].

[4] The present study is motivated by several factors that contribute to improved characterization of seismicity in this area, coupled with more detailed crustal models than were previously available. The advent of the POLARIS network [*Eaton et al.*, 2005] and recent expansion

[1]Department of Earth Sciences, University of Western Ontario, London, Ontario, Canada.

0148-0227/07/2006JB004827$09.00

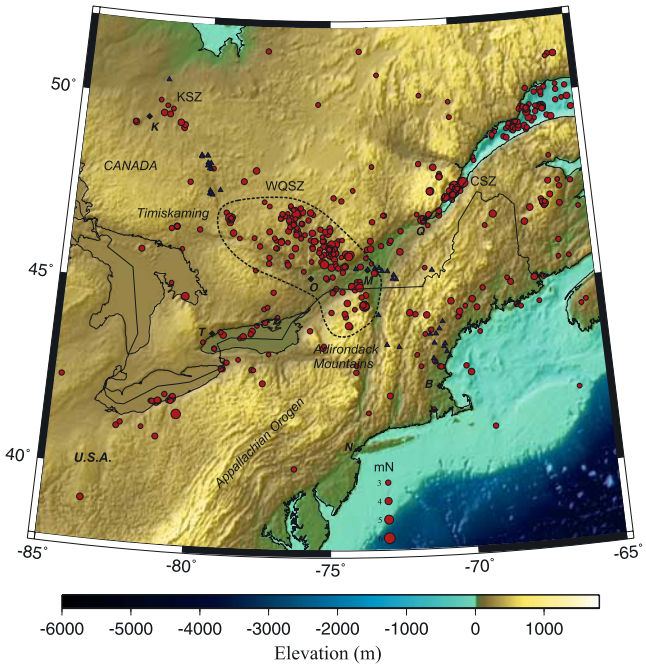

Figure 1. Distribution of earthquakes in southeastern Canada and northeastern United States with mN $\geq$ 2.7, from 1995–2006 (source Earthquakes Canada online catalog, http://earthquakescanada.nrcan.gc.ca). Diamonds indicate locations of cities: Kapuskasing (K), Ottawa (O), Montreal (M), Quebec (Q), Toronto (T), Boston (B), and New York (N). WQSZ denotes the western Quebec seismic zone; CSZ denotes Charlevoix seismic zone; KSZ denotes Kapuskasing seismic zone. The small triangles show locations of igneous intrusions interpreted to be caused by the Great Meteor hot spot. The figure was prepared using the GMT software [*Wessel and Smith*, 1998].

of the Lamont-Doherty Cooperative Seismographic Network (LCSN) have augmented seismic network coverage in this region, providing improved observational constraints on recent seismicity. In addition, development and refinement of the regional depth phase modeling method [*Ma et al.*, 2003; *Ma and Atkinson*, 2006] has enabled the determination of earthquake focal depths with much greater accuracy than was previously possible. Finally, a high-quality crustal-scale vibroseis profile acquired by Canada's LITHOPROBE program [*Martignole and Calvert*, 1996] is situated within the WQSZ along most of its length, providing a new geological framework for interpreting the regional seismicity.

[5] The objectives of this study are threefold. First, by compiling published results for the WQSZ and combining these with new observations, our aim is to characterize several key source parameters (focal depths and focal mechanism) and their spatiotemporal clustering. Second, through detailed comparison of hypocenter locations with a composite LITHOPROBE seismic profile through the WQSZ and other geological data, our objective is to test hypotheses for underlying tectonic controls on earthquake locations. These hypotheses include (1) reactivation of antecedent fault zones, including Mesoproterozoic shear zones associated with the Grenville orogeny [*Forsyth*, 1981] and/or late Precambrian and early Paleozoic normal faults associated with opening of the Iapetus ocean [*Adams and Basham*, 1991; *Bent et al.*, 2002], and (2) localization of seismicity along the Mesozoic track of the Great Meteor hot spot [*Adams and Basham*, 1991], possibly due to strength contrasts between mafic intrusions and felsic rocks in the middle crust [*Dineva et al.*, 2007]. We also critically evaluate the hypothesis that microearthquake clusters represent exceptionally long-lived aftershock clouds from large prehistoric earthquakes [*Ebel et al.*, 2000; *Ma and Atkinson*, 2006].

2. Historical Seismicity

[6] The largest historical earthquake in the WQSZ is the M = 6.2, 1 November 1935 Timiskaming earthquake (Figure 2a). This earthquake was felt over a large area of eastern North America, from the west end of Lake Superior to the Atlantic, and as far south as Kentucky and Virginia [*Doig*, 1991; *Bent*, 1996b]. In the epicentral region, a maximum MMI intensity of VII is indicated by extensive property damage, especially to chimneys [*Hodgson*, 1936a, 1936b]. Effects on the surrounding landscape included rockfalls and discoloration of a lake by resuspension of freshwater mud and organic matter [*Doig*, 1991]. On 1 January 2000 the mN = 5.2 Kipawa earthquake occurred close to the epicenter of the 1935 earthquake and was felt to a radius of 500 km [*Bent et al.*, 2002]. (The notation mN denotes Nuttli magnitude [*Nuttli*, 1973] applied to high-frequency observations, as used by Earthquakes Canada for its catalog of seismicity. Note that such mN magnitudes tend to be somewhat greater (by ~0.5) than those found using other common magnitude scales for moderate earthquakes.) Much earlier, in September 1732 a strong earthquake (M_L5.8) occurred near Montreal. About 300 houses were damaged, many chimneys were tumbled down, and people were wounded with one possible fatality [*Smith*, 1962; *Leblanc*, 1981].

[7] Several more recent earthquakes are also notable. The M_W = 5.6 Cornwall-Massena earthquake on 5 September 1944 caused considerable damage [*Hodgson*, 1945; *Bent*, 1996a]. Inversion of regional waveform recordings show that this event occurred in the midcrust (~20 km) with an oblique thrust mechanism, similar to the mechanism for other events in the WQSZ and consistent with the regional stress field [*Bent*, 1996a]. On 20 April 2002, a M_W 5.0 earthquake occurred near the town of Au Sable Forks in the Adirondack mountains of New York [*Seeber et al.*, 2002], causing damage to roads, bridges, the power system, water lines, and residential houses [*Pierre and Lamontagne*, 2004]. Ground motion from this event was exceptionally well recorded by recently expanded seismograph networks in this region [*Atkinson and Sonley*, 2003].

[8] On a more regional scale, large historical earthquakes have occurred within the St. Lawrence valley in the Charlevoix seismic zone, northeast of Quebec City (Figure 2a). This is the most active seismic zone in eastern Canada [e.g., *Buchbinder et al.*, 1988], with a record of major historical earthquakes in 1663 ($M \sim 7$ [*Basham et al.*, 1979]), 1791 ($M \sim 6$), 1860 ($M \sim 6$), 1870 ($M \sim 6.5$) and 1925 ($M \sim 6.2$). The most recent significant earthquake near this zone was the M_W = 5.9 Saguenay earthquake on 25 November

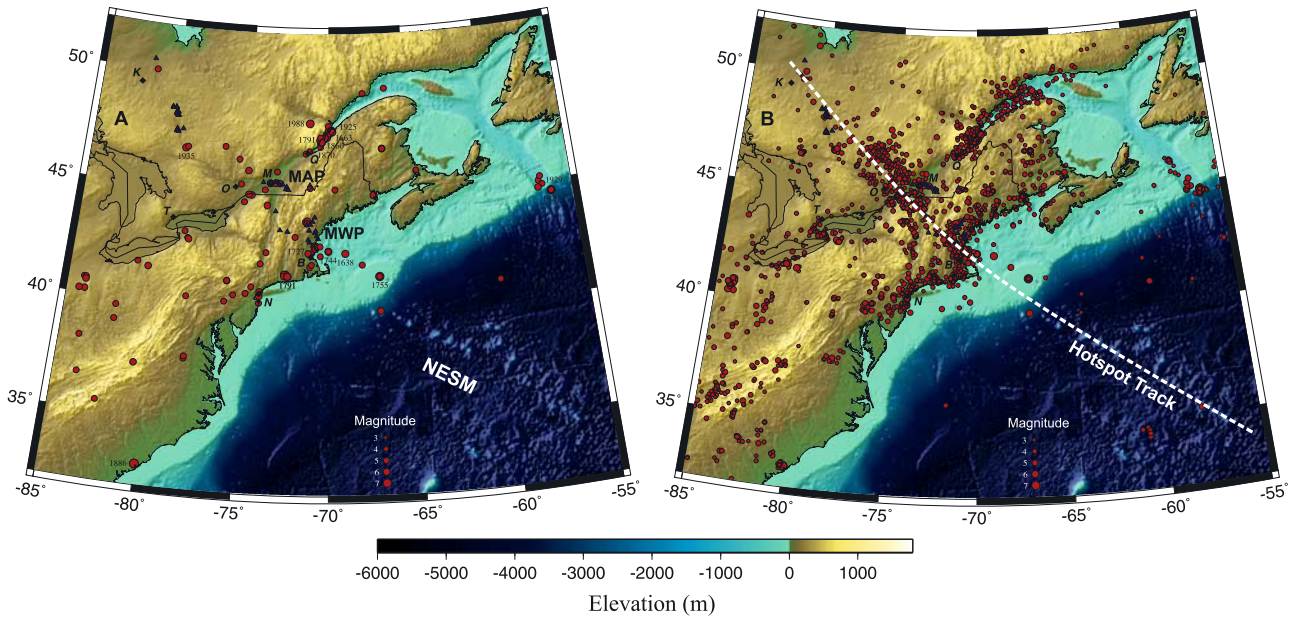

Figure 2. (a) Distribution of earthquakes with estimated magnitude ≥ 5 in eastern North America from 1663 to 2006 (source USGS online catalog), showing ages for significant historical events described in the text. Triangles show locations of igneous intrusions interpreted to be caused by the Great Meteor hot spot, including 146 ± 8 Ma kimberlites (K [*Heaman and Kjaarsgaard*, 2000]), 129 ± 9 Ma Monteregian alkaline plutons (MAP [*Eby*, 1984]); and 115 ± 7 Ma Mount White plutons (MWP [*Zartman*, 1977]). The Great Meteor hot spot track is evident from the locations of the New England seamount trend (NESM). (b) Distribution of earthquakes with estimated magnitude ≥ 3 from 1568 to 2006. The dashed line shows the hot spot track; the WQSZ is along the track. Cities are marked as in Figure 1.

1988, the largest earthquake in eastern North America for over half a century [*Haddon*, 1995].

[9] Paleoseismic evidence, in the form of giant landslides and severely disturbed ground in Champlain Sea sediments east of Ottawa, suggests that large prehistoric earthquakes have occurred in the WQSZ [*Aylsworth et al.*, 2000]. Radiocarbon ages of wood and plant materials indicate that the disturbances were caused by two separate events, circa 4550 years B.P. and circa 7060 years B.P. Comparison of the extent and intensity of ground disturbance with the paleoseismic record of other large regional events suggests that these prehistoric earthquakes were both comparable in magnitude to the M $\sim$ 7 1663 Charlevoix earthquake [*Aylsworth et al.*, 2000].

[10] Examination of the distribution of historical seismicity in eastern North America (Figure 2) suggests that events are generally concentrated within a few distinct bands of activity. This impression is reinforced when all known historical events with magnitude $\geq$ 3 are considered (Figure 2b). Two, margin-parallel, NE striking bands of earthquakes are evident, along the St. Lawrence valley and Appalachian Mountains, respectively. In addition, a NW striking band of seismicity extends into North America, continuing the trend of the New England seamounts and consistent with locations of kimberlite intrusions and other igneous activity along the inferred continental track of the Great Meteor hot spot [*Heaman and Kjaarsgaard*, 2000] (Figure 2). *Sykes* [1980] was the first to propose that regional seismicity may be localized along the hot spot track. In the Boston region a number of large historical events occurred along this trend, in both onshore and offshore regions during the 17th and 18th centuries, including the 1755 Cape Ann *M*6.2 earthquake [*Ebel*, 2002], the 1727 *M*7 [*Ebel*, 2000], and 1638 *M*6.5 [*Ebel*, 1998] in Boston-Concord region.

3. Tectonic Setting

[11] The generalized geology of the study region is shown in Figure 3. Tectonic elements in this region were formed over a long time interval spanning a substantial fraction of Earth history, from > 2.8Ga within the Superior Province (Laurentian craton) to 115 Ma intrusions along the track of the Great Meteor hot spot. The two major orogenic belts that transect the region are the Mesoproterozoic Grenville orogeny and the Silurian-Permian Appalachian orogeny [*Faill*, 1997]. In our study region, both of these belts are approximately parallel to the eastern margin of North America.

[12] The 1.2–0.98 Ga Grenville orogeny was one of the most extensive mountain-building episodes in Earth history. Although it is primarily exposed within the Canadian Shield, the Grenville orogeny continues in the subsurface beneath Phanerozoic sedimentary rocks of the interior platform (Figure 3). The scale and tectonic architecture of the Grenville orogeny resemble the modern Alpine-Himalayan orogeny, suggesting that it formed as the result of broadly similar continent-continent collisional processes [*Carr et al.*, 2000]. Several recent tectonic models also emphasize the precollisional history of the orogen, during which an Andean-style convergent margin persisted for almost 800 Ma along the southeastern margin of the North American protocontinent, Laurentia [*Rivers*, 1997]. Crustal

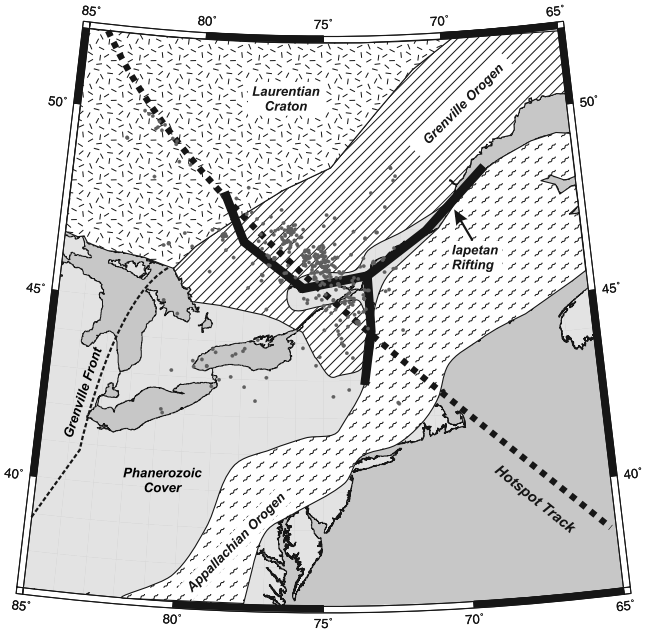

Figure 3. Generalized geology of the study region, after *Faill* [1997], showing earthquake epicenters from Figure 1. Two large orogenic belts cut across the region, the 1.2–1.0 Ga Grenville orogeny, and the 460–260 Ma Appalachian orogeny. Heavy lines denote failed rift arms, which are characterized by normal faults and mafic dikes emplaced during incipient opening of the Iapetus Ocean, circa 650 Ma. The dashed line shows the approximate inferred track of the Great Meteor hot spot over the time interval from circa 180 Ma (in the northwest) to circa 110 Ma beneath the Atlantic Ocean [see *Heaman and Kjaarsgaard*, 2000].

thickness within the Grenville province varies between 30 and 48 km, with generally thinner crust in the vicinity of the WQSZ [*Eaton et al.*, 2006].

[13] The Iapetus Ocean formed ~ 420 Ma during the breakaway of Laurentia from the supercontinent Gondwana [*Prigmore et al.*, 1997]. Extension and rifting associated with incipient opening of Iapetus began as early as 650 Ma, and resulted in the creation of normal faults and mafic dike emplacement along the Ottawa-Bonnechere graben system [*Kamo et al.*, 1995]. Closure of the Iapetus Ocean and subsequent continent-continent collision to form the supercontinent Pangea produced widespread orogenesis in North America and Europe. In eastern North American, the 3000+ km long Appalachian orogen formed as the result of separate continental collisions during the assembly of Pangea, including the Ordovician-Silurian Taconic orogeny, the Middle and Late Devonian Acadian orogeny, and the Permian Allegheny orogeny (see review by *Faill* [1997]). Crustal extension in the Late Triassic and Early Jurassic produced igneous activity and numerous local, closed basins along the eastern margin of North America [*Faill*, 1997].

[14] The Great Meteor (also known as New England or Monteregian) hot spot track in the Atlantic and North America has been studied extensively [e.g., *Crough*, 1981; *Morgan*, 1983; *Sleep*, 1990]. Igneous crystallization ages increase monotonically along the track [*Heaman and Kjaarsgaard*, 2000] and are generally consistent with the hot spot model, although alternative interpretations of parts of the track have been proposed [*McHone*, 1996]. Surface features attributed to the hot spot include small-volume kimberlite eruptions that originate in the upper mantle and penetrate through thick lithosphere in the interior of the craton [*Heaman and Kjaarsgaard*, 2000], intermediate-volume alkaline magmas that occur near the edge of the craton and within the Appalachian orogeny [*Zartman*, 1977; *Eby*, 1984]. This progressive change in the inferred near-surface expression of the hot spot suggests a systematic evolution from kimberlitic melts to more voluminous crustal magmatism, as the inferred hot spot interacted with a progressively thinner lithosphere due to motion of the overriding plate.

4. Focal Depth Estimation

[15] *Ma and Atkinson* [2006] have computed focal depths for 328 events in the WQSZ and surrounding areas, using a regional depth phase modeling (RDPM) method. The results of their work are important here, since earthquake hypocenters in the WQSZ are generally deeper than surrounding background seismicity, and because the improved depth resolution allows us to make direct comparisons of the hypocenter distribution with other geophysical data (see below). Here, we briefly summarize the method and present an updated set of measurements for this region.

[16] The RDPM method requires the identification of a regional depth phase, such as *sPg*, *sPmP*, *sPn*, and its corresponding reference phase (*Pg*, *PmP*, *Pn*). The choice of depth phase is dependent on the epicentral distance; in this region, for stations in the distance range of 78 to 120 km the most prominent depth phase is *sPg*, for stations at distances from 192 to 234 km the most prominent depth phase is *sPmP*, and for stations at distances from 426 to 597 the most prominent depth phase is *sPn* [*Dineva et al.*, 2007]. The estimated focal depth depends on the time difference between these two respective phases, which, for a given velocity model, depends almost entirely on focal depth. To improve the accuracy of the method over manual time picking, a visual comparison is made between observed seismograms and synthetics calculated by a standard algorithm such as reflectivity [e.g., *Randall*, 1994]. Figure 4 shows an example of a RDPM comparison for an event in the WQSZ, using the depth phase *sPmP*.

[17] In this study, we have augmented the focal depths computed by *Ma and Atkinson* [2006] with an additional 73 depth-located events. Our combined results are summarized in Figure 5, which shows the distribution of earthquakes in the WQSZ subdivided by focal depth. For focal depths < 8 km (Figure 5a), earthquakes are distributed in an apparently random fashion throughout the region. For focal depths between 8 and 17 km (Figure 5b), we observe a well defined linear band of earthquakes in the WQSZ. For focal depths deeper than 17 km (Figure 5c), earthquake epicenters are more localized and appear to define distinct clusters. Parameters for the 73 events determined in this study are tabulated in Table 1.

5. Waveform Fitting and Focal Mechanisms

[18] Using regional waveform recordings, we have calculated a best fitting double-couple mechanism for a recent

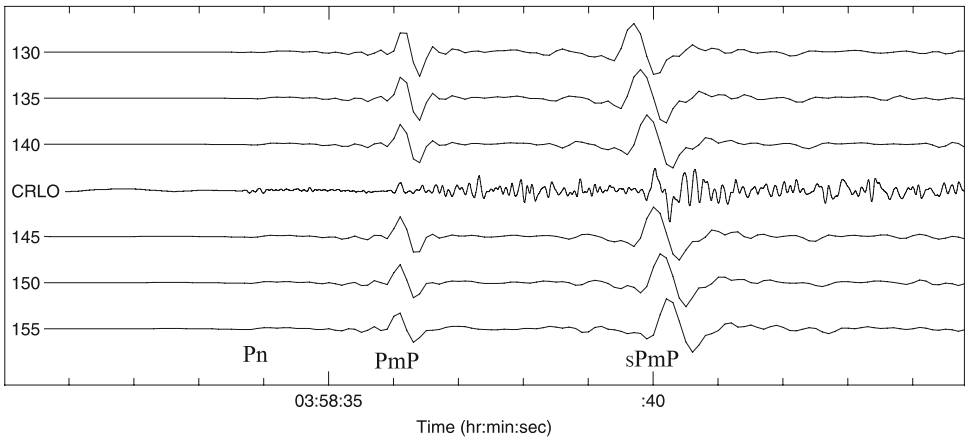

Figure 4. Example of earthquake focal depth determination using the regional depth phase modeling (RDPM) method. The focal depth for this event is estimated to be between 14.0 and 14.5 km. The comparison is between synthetics generated with an earthquake source model and the P portion recorded at station CRLO generated by a small earthquake (12 September 1995, mN 3.7; in west Quebec). The first trace 130 was generated with depth 13 km, at distance 2.10° and azimuth 283°. Traces 135, 140, 145, 150, and 155 were generated with depths 13.5, 14.0, 14.5, 15.0, and 15.5 km, respectively. Other parameters are the same as those for trace 130.

moderate (mN = 4.5) earthquake that occurred northeast of Ottawa on 25 February 2006. We use a waveform-fitting procedure that solves for double-couple parameters and station-dependent time shifts. In contrast to similar studies that have relied mainly on long-period surface waveforms [e.g., *Kim et al.*, 2006], our inversion procedure uses primarily body waves, since the focal depth of this event is too large for such a small earthquake to produce strong surface waves [*Saikia*, 1992]. Our method also uses user-specified time windows around the phases of interest and allows for mutually independent time shifts. The waveform fitting process is carried out using synthetic seismograms, denoted by the vectors $m_{11}(t)$, $m_{22}(t)$, $m_{33}(t)$, $m_{12}(t)$, $m_{13}(t)$, and $m_{23}(t)$, which are computed for six elementary moment tensor components (M_{11}, M_{22}, M_{33}, M_{12}, M_{13}, M_{23}) using the wave number integration method of *Herrmann* [2002]. For a particular set of double-couple parameters (strike angle θ, dip δ and rake λ) and seismic moment M_0, a synthetic three-component seismogram $s(t)$ is obtained using the formula

$$\begin{aligned} s(t) = M_0[&2n_1d_1m_{11}(t) + 2n_2d_2m_{22}(t) + 2n_3d_3m_{33}(t) \\ &+ (n_1d_2 + n_2d_1)m_{12}(t) + (n_1d_3 + n_3d_1)m_{13}(t). \\ &+ (n_2d_3 + n_3d_2)m_{23}(t)], \end{aligned} \quad (1)$$

where

$$n = [n_1, n_2, n_3] = [-\sin\delta\sin\theta, -\sin\delta\cos\theta, \cos\delta] \quad (2)$$

is the normal vector to one of the nodal planes and

$$\begin{aligned} d &= [d_1, d_2, d_3] \\ &= [\cos\lambda\cos\theta + \sin\lambda\cos\delta\sin\theta, -\cos\lambda\sin\theta \\ &\quad + \sin\lambda\cos\delta\cos\theta, \sin\lambda\sin\delta] \end{aligned} \quad (3)$$

is the corresponding slip vector direction [*Stein and Wysession*, 2003]. We use a velocity model applicable to western Quebec [*Mereu et al.*, 1986], along with a triangular source pulse 0.3 s in duration. Both the observed and synthetic seismograms were filtered using a fourth-order Butterworth filter with a passband of 0.4 to 4.0 Hz. The best fitting parameters were obtained by a weighted least squares method, using an exhaustive search over a user-specified range of M_0 values and the full parameter space of $0° \le \theta \le 360°$, $0° \le \delta \le 90°$ and $-90° \le \lambda \le 270°$.

[19] Figure 6 shows the lower hemispherical projection of our best double-couple solution for the 25 February 2006 earthquake, as well as a waveform comparison between the observed and synthetic seismograms generated using this focal mechanism solution. The double-couple parameters for this event are summarized in Table 2. The fit between the observed and synthetic waveforms is generally good (Figure 6). We remark that this earthquake location (Figure 5c) is not far from several postulated large prehistoric earthquakes [*Aylsworth et al.*, 2000].

[20] Figure 7 shows a compilation of our new result along with 13 representative focal mechanisms for moderate-sized earthquakes in this region, for which published waveform modeling solutions are available. The parameters used to generate Figure 7 are listed in Table 3. All events in the WQSZ have a reverse-sense focal mechanism, although some spatial variability is apparent. For example, earthquakes north of $\sim 45°$ have a NE-SW oriented P axis, whereas two events in the Adirondack region in the southeastern part of the zone have E-W oriented P axis [*Nabelek and Suarez*, 1989; *Seeber et al.*, 2002; *Ma and Adams*, 2002]. Furthermore, as noted by *Kim et al.* [2006], events in Lake Ontario and south of the Great Lakes are mainly of strike-slip character but have a very similar P axis orientation to reverse-sense focal mechanisms in the WQSZ. A recent event in Georgian Bay also has a focal mechanism very similar to those in the WQSZ [*Dineva et al.*, 2007],

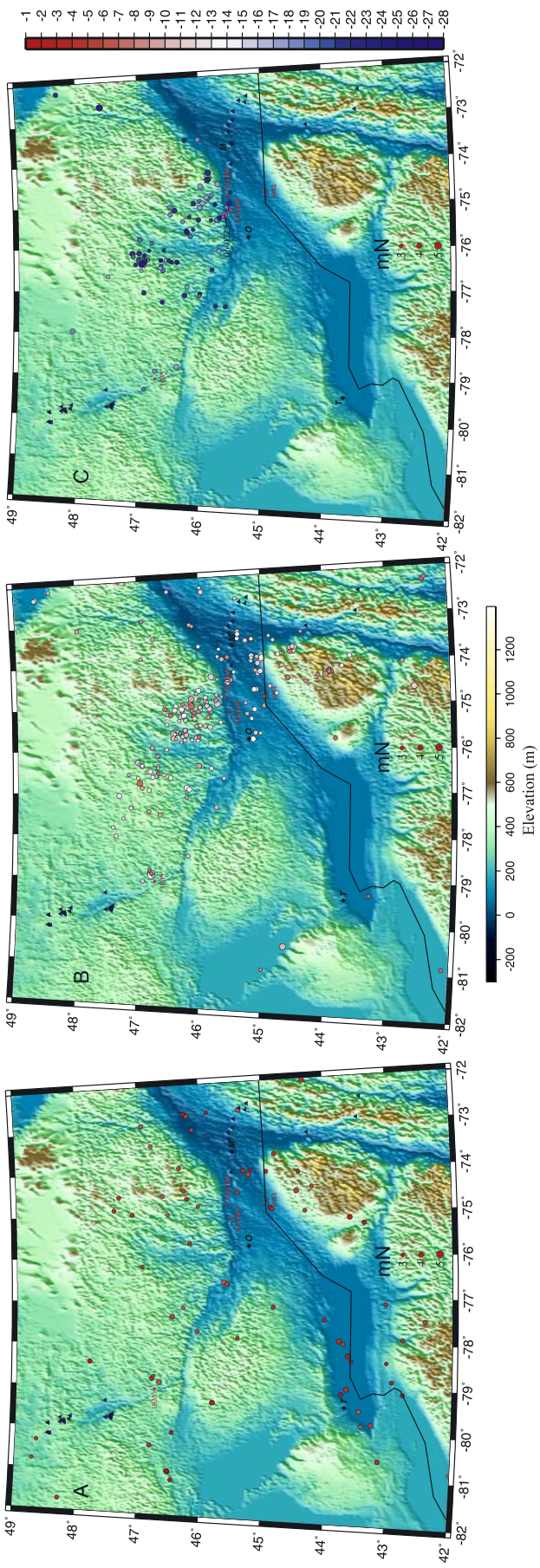

Figure 5. Distribution of earthquakes (mN $\geq$ 2.8) in the WQSZ and surrounding area. (a) Distribution of earthquakes with focal depths shallower than 8 km. The events are scattered in an apparently random fashion throughout the region. (b) Distribution of earthquakes with focal depths between 8 and 17 km (inclusive). In this case, the events are concentrated within a well defined linear band (the WQSZ). (c) Distribution of earthquakes with focal depths deeper than 17 km. These deep events are confined to a few distinct clusters within the WQSZ. The solid circle with red star shows the epicenter of 25 February 2006 mN 4.5 earthquake. The color pallet on the right shows the focal depth range in km.

Table 1. Catalog of Events in the WQSZ for Which Focal Depths Have Been Determined in This Study

Event	Date[a]	Time, UT	Latitude	Longitude	h, km	mN[b]
1	1983/12/28	1224:21	47.07	−76.28	16.0	3.5
2	1984/06/07	0933:54	46.11	−75.44	10.0	2.9
3	1987/01/22	2057:16	46.97	−76.32	26.0	2.9
4	1987/12/20	0752:48	48.66	−80.34	04.5	2.7
5	1988/03/10	1442:55	46.34	−75.67	17.0	3.7
6	1988/03/11	0640:42	47.03	−76.38	22.0	2.4
7	1989/01/10	1841:27	46.34	−75.68	16.0	2.9
8	1991/04/28	0413:16	46.91	−76.24	19.0	2.4
9	1992/08/11	1950:44	48.72	−80.79	06.0	2.5
10	1992/08/21	1522:41	46.34	−75.37	19.0	3.1
11	1993/05/29	1048:05	46.17	−75.56	22.0	2.8
12	1993/10/09	2116:21	46.96	−76.31	18.0	3.4
13	1994/01/31	0109:48	47.05	−76.27	20.0	2.1
14	1995/06/04	2129:40	47.02	−76.29	22.0	2.7
15	1996/04/20	0143:03	49.18	−80.97	05.0	3.3
16	1996/08/16	0456:46	49.24	−82.95	04.5	3.7
17	1996/08/22	2019:06	49.25	−82.97	04.5	2.8
18	1997/01/05	0753:17	46.42	−75.55	10.0	2.5
19	1997/03/15	0801:17	46.45	−75.73	11.0	2.4
20	1997/06/23	0214:18	47.04	−76.33	17.0	2.6
21	1998/02/02	0136:04	47.04	−76.25	24.0	2.3
22	1999/02/01	2222:05	49.26	−80.94	13.0	3.4
23	1999/04/26	1344:27	46.47	−75.62	14.0	2.4
24	2000/01/14	1214:24	46.96	−76.25	22.0	2.5
25	2000/11/05	1614:03	49.67	−81.47	10.0	2.7
26	2001/01/09	1623:58	50.00	−82.34	09.0	2.5
27	2001/06/12	2040:31	47.00	−76.35	15.0	2.7
28	2001/09/09	0601:30	46.99	−76.32	25.0	2.0
29	2001/09/29	1230:14	47.01	−76.24	19.0	2.1
30	2001/10/27	1707:49	46.91	−76.27	19.0	2.2
31	2005/01/30	1806:45	48.13	−77.97	19.0	3.8
32	2005/02/26	1112:14	46.53	−80.99	01.0	2.9
33	2005/03/03	0222:01	45.06	−74.20	13.0	3.5
34	2005/03/13	1708:14	46.54	−80.98	03.0	3.6
35	2005/03/28	1639:38	43.33	−79.28	09.5	3.1
36	2005/03/28	1658:28	43.32	−79.28	08.0	2.8
37	2005/03/31	1513:08	46.28	−75.64	11.0	3.4
38	2005/04/08	0432:38	46.27	−73.46	22.0	3.3
39	2005/05/25	1922:13	46.27	−75.62	24.0	3.7
40	2005/05/31	1349:04	44.97	−74.07	04.0	2.9
41	2005/06/23	1816:21	46.06	−75.05	18.0	3.0
42	2005/06/23	1816:24	46.04	−75.04	18.0	2.9
43	2005/06/23	1832:08	46.06	−75.05	18.0	3.3
44	2005/07/04	1147:13	46.24	−76.91	15.0	3.6
45	2005/07/10	0451:07	46.48	−81.18	03.0	3.1
46	2005/07/23	0248:16	47.04	−75.79	20.0	3.5
47	2005/07/27	1124:32	45.41	−73.34	14.0	3.2
48	2005/08/04	2319:46	46.19	−75.76	12.0	2.5
49	2005/09/06	0258:45	45.72	−75.36	13.0	2.9
50	2005/09/06	1410:51	46.28	−75.29	17.0	3.5
51	2005/09/21	0336:31	46.54	−80.98	02.0	2.9
52	2005/10/01	0701:44	46.71	−76.45	18.0	3.0
53	2005/10/20	2116:28	44.68	−80.48	11.0	4.3
54	2005/10/25	1529:04	46.82	−78.86	17.0	3.3
55	2005/11/19	1318:53	47.15	−76.18	20.0	3.1
56	2006/01/03	1105:10	49.32	−81.12	22.0	3.7
57	2006/01/09	1535:39	45.03	−73.90	15.0	4.2
58	2006/02/07	0407:21	46.29	−75.30	16.0	3.1
59	2006/02/25	0139:22	45.66	−75.24	19.0	4.5
60	2006/02/26	0409:22	45.55	−74.71	22.0	3.1
61	2006/03/04	0213:10	49.52	−81.58	16.0	3.4
62	2006/03/04	1820:03	46.84	−78.89	08.0	2.8
63	2006/04/07	1244:26	46.83	−76.62	15.0	3.1
64	2006/05/11	0635:38	46.27	−72.68	03.0	3.1
65	2006/05/21	0716:17	46.39	−75.31	16.0	2.8
66	2006/06/05	1744:23	49.92	−82.16	08.0	2.5
67	2006/10/10	0620:28	43.90	−73.32	05.0	2.9
68	2006/11/10	2351:37	46.17	−76.84	05.0	2.9
69	2006/11/29	0738:17	46.48	−81.21	02.5	3.1
70	2006/11/29	0736:17	46.47	−81.22	02.5	2.0
71	2006/11/29	0722:55	46.48	−81.18	02.5	4.1
72	2006/12/07	0444:59	49.52	−81.54	15.0	4.2
73	2007/01/06	0408:44	47.03	−76.23	22.0	3.3

[a]Date format is year/month/day.
[b]Nuttli magnitude [*Nuttli*, 1973], as reported by Earthquakes Canada in its online catalog of seismicity.

narrowing the distance range over which the change from reverse to strike slip faulting occurs.

6. Spatial Clustering of Earthquakes

[21] While the foregoing discussion provides a description of the patterns of seismicity, it is useful to take a more quantitative approach in order to mitigate interpretive bias. To this end, we have developed a statistical approach to characterize spatial clustering of seismicity. The epicenters and magnitudes determined by Canadian National Seismograph Network for this analysis includes all events listed in the Earthquakes Canada online catalog for the period 1 January 1980 to 1 June 2006 in the area 42°N–49°N, 72°W–82°W. We selected 1980 as a starting time for the analysis, since location uncertainties for pre-1980 events tend to be large due to the sparse distribution of seismograph stations in that time.

[22] As an initial step in the procedure, we determined a magnitude threshold for catalog completeness using a cumulative Gutenberg-Richter plot (Figure 8). The circles in Figure 8 denote the average number of events per year with magnitude greater than or equal to a certain value. Error bars indicate ± one standard deviation from the average, obtained by repeating the calculation for 27 years on a calendar year basis. In the cases where the standard deviation is greater than the mean value, the number of events per year is not statistically different from zero at the 68% confidence level and the lower uncertainty limited is represented as a dashed line. This approach suggests that the GSC catalog for this region and time interval can be considered as complete for magnitudes greater than $\sim$ mN 2. Thus the following clustering analysis is limited to events greater than this magnitude.

[23] A point distribution is said to be clustered if the points are concentrated within localized regions of the attribute space [*Swan and Sandilands*, 1995]. To test for spatial clustering, we used a χ^2 test for randomness. The test is preformed by subdividing the area of interest into square cells, counting the number of points that fall within each cell, and constructing a histogram. In the case that the point data have statistically random spatial distribution, the histogram is expected to resemble a Poisson distribution:

$$P_v(n) = v\left(\frac{N}{v}\right)^n \frac{1}{n!} e^{\frac{-N}{v}} \tag{4}$$

where, for a random distribution of epicenters, $Pv(n)$ is the expected number of bins containing n events, v is the number of bins in the study region and N is the number of epicenters in the catalog. The bin size is a free parameter that determines v and also affects the distribution; in order

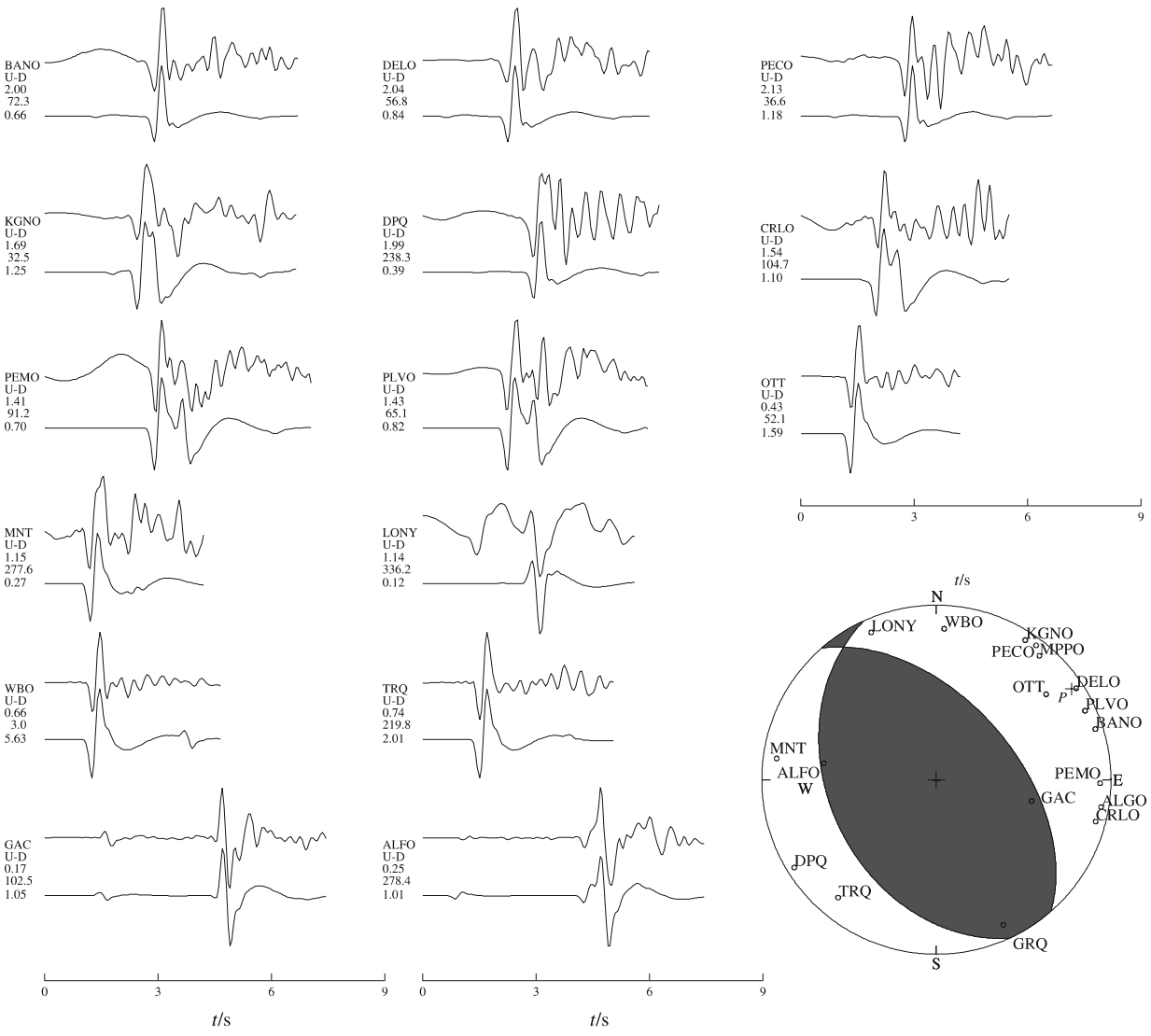

Figure 6. Waveform comparison and inferred focal mechanism for the 25 February 2006 mN 4.5 earthquake northeast Ottawa. For each pair of waveforms, the upper trace is the recorded waveform; the lower trace is the synthetic generated with the focal mechanism solution. Both the observed and the synthetic were filtered with passband 0.4 $\sim$ 4 Hz. At the left side of each pair the symbols and numbers from top to bottom indicate station name, vertical component, distance in degree, station azimuth in degree, and the ratio between observed maximum amplitude and that of the synthetic. The lower hemispherical projection of the focal mechanism is at the bottom right corner. The symbols are station names.

for the statistical test to be valid, the dimensions of the bin must be significantly larger than the uncertainty in epicentral location but significantly smaller than the total area of the study. We have tested bin sizes in a range from 10 km to 50 km, which satisfies these conditions, and although the details differ all of these bin sizes support a similar interpretation of the results. Figure 9 shows the curves obtained using a 15 km $\times$ 15 km bin size. Relative to a Poisson distribution (dashed line Figure 9), the curve shows a deficiency of bins with 1–3 events, whereas bins with 4 or more events are more abundant than expected based on a Poisson distribution. Here, we define this

Table 2. Double-Couple Source Parameters for the 25 February 2006 Earthquake Northeast of Ottawa[a]

Parameter	Value
M_0	$3.5 \pm 1.1 \times 10^{14}$N m
M_W	3.7 ± 0.1
S_1, S_2	$319 \pm 15°$,$155 \pm 15°$
D_1, D_2	$53 \pm 8°$, $38 \pm 8°$
R_1, R_2	$80 \pm 18°$, $103 \pm 18°$
Paz, Pp	$56 \pm 16°$, $8 \pm 14°$
Taz, Tp	$188 \pm 16°$, $80 \pm 16°$

[a]S_1, D_1, R_1, and S_2, D_2, R_2 denote the strike, dip, and rake for nodal planes 1 and 2, respectively. Paz, Pp, and Taz, Tp denote the azimuth and plunge for the principle axes (P and T), respectively.

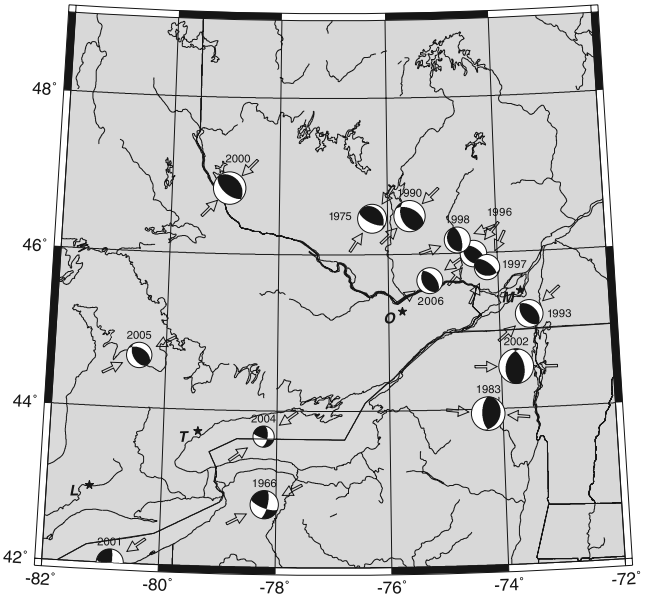

Figure 7. Selected focal mechanism solutions for earthquakes in the WQSZ and surrounding region. The solutions are mainly for moderate and submoderate earthquakes; they were selected from the following sources: *Dineva et al.* [2007], *Du et al.* [2003], *Herrmann* [1978], *Horner et al.* [1978], *Kim et al.* [2006], *Ma et al.* [2002], and *Nabelek and Suarez* [1989]. The focal mechanism parameters used to generate the image are listed in Table 3. The arrows show the P axis direction.

crossover point along the curves as the events-per-bin threshold value that separates seismicity that is clustered from areas of random background seismicity.

[24] Figure 10a shows a contour map of the spatial density of cataloged seismicity, computed using a bin size of 15km × 15 km. The seismicity used in this analysis is plotted in Figure 10b. The first contour level in Figure 10a represents four events per bin, based on our criterion for exceedance of random background seismicity. The lowest contour level can thus be interpreted to enclose spatial clusters of seismicity. We have named the largest WQSZ clusters identified using this approach as follows: Timiskaming, Maniwaki, Mont Laurier and Adirondack. We remark that the Timiskaming cluster is located close to the epicenter of the 1935 Timiskaming earthquake, and a smaller unnamed cluster, 60 km west of the Adirondack cluster, is located adjacent to the epicenter of the 1944 Cornwall-Massena earthquake. Furthermore, the Mont Laurier cluster, which is characterized by two local maxima in spatial density of cataloged seismicity, is adjacent to locations where paleoseismic evidence suggests that large prehistoric earthquakes may have occurred [*Aylsworth et al.*, 2000].

[25] To characterize the seismicity of each cluster, we have computed the *b* parameter (slope) from the Gutenberg-Richter graphs for individual clusters (Figure 11), as well as the area of the cluster enclosed within the random exceedance contour (Figure 10a). The *b* value and associated uncertainties were calculated using the maximum-likelihood method of *Aki* [1965], yielding values in the range 0.56–

Table 3. Earthquakes With Published Focal Mechanisms Used in Figure 7[a]

Date	Latitude, °N	Longitude, °W	Depth	Moment, 10^{21}dyn cm	Mw	Nodal Planes, deg			P Axis Az/PL	T Axis Az/PL	Location	References
						Strike	Dip	Rake				
1966/01/01	42.80	78.20	2	13	4.1	13	71	159	62/1	331/28	Attica, New York	*Herrmann* [1978]
						110	70	20				
1975/07/12	46.46	76.28	17	17	4.4	116	65	79	214/19	5/68	Maniwaki, Quebec	*Horner et al.* [1978]
						326	21	112				
1983/10/07	43.94	74.26	7.5	190	4.85	180	61	81	277/16	68/72	Goodnow, New York	*Nabelek and Suarez* [1989]
						18	30	106				
1990/10/19	46.49	75.59	12	57.8	4.5	158	45	121	47/4	146/68	Mont Laurier, Quebec	*Ma and Adams* [2002]
						298	52	62				
1993/11/16	45.20	73.46	12	8.2	3.9	144	45	96	50/0	142/86	Napierville, Quebec	*Du et al.* [2003]
						316	45	84				
1996/03/14	45.99	74.43	18	4.6	3.7	136	36	98	40/9	191/80	Lachute, Quebec	*Du et al.* [2003]
						306	54	84				
1997/05/24	45.81	74.19	22	3.2	3.6	96	33	60	27/15	256/68	Christieville, Quebec	*Du et al.* [2003]
						311	62	108				
1998/07/30	46.17	74.72	12	4.4	3.7	150	27	75	71/19	272/70	Laconception, Quebec	*Du et al.* [2003]
						347	64	98				
2000/01/01	46.84	78.93	13	104.1	4.7	320	33	99	224/12	21/77	Kipawa, Quebec	*Ma and Adams* [2002]
						130	57	84				
2001/01/26	41.99	80.83	2	7.5	3.9	5	79	159	53/7	320/23	Ashtabula, Ohio	*Du et al.* [2003]
						99	69	12				
2002/04/20	44.53	73.73	10	335.8	5.0	196	40	111	91/7	207/75	Plattsburgh, New York	*Ma and Adams* [2002]
						349	53	73				
2004/08/04	43.67	78.23	4	0.445	3.1	106	77	32	234/12	331/31	Port Hope, Lake Ontario	*Kim et al.* [2006]
						8	59	165				
2005/10/20	44.67	80.48	12	2.67	3.6	299	45	68	242/2	127/75	Georgian Bay, Ontario	*Dineva et al.* [2007]
						149	49	110				
2006/02/25	45.66	75.24	19	3.5	3.7	319	53	80	56/8	188/80	Buchingham, Quebec	this paper
						155	38	103				

[a]Az, azimuth; PL, plunge; both in degrees.

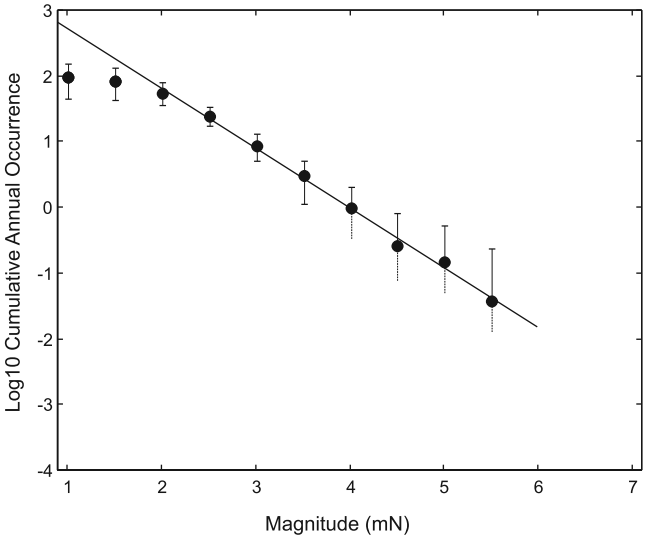

Figure 8. Gutenberg-Richter plot using cumulative seismicity for the region 42°–49°N and 82°–72°W for the period 1 January 1980 to 1 June 2006 (source Earthquakes Canada online catalog, http://earthquakescanada.nrcan.gc.ca). This graph shows that the catalog can be considered to be complete for magnitude mN > 2.

0.87. With this method the *b* value for the entire region is 0.834, with uncertainties of 0.028, 0.036 and 0.043 at the 80%, 90% and 95% confidence levels, respectively. It should be stressed that since the number of events in each cluster is relatively small, we expect a high level of uncertainty in these derived parameters. Nevertheless, we find that there are statistically significant variations in seismicity parameters that characterize each cluster. These parameters are summarized in Table 4 and discussed below.

7. Repeating Earthquakes

[26] We have carefully analyzed waveform records from one of the clusters (the Maniwaki cluster) in more detail than the others and found evidence for repeating earthquakes [*Schaff and Richards*, 2004]. These represent multiple events, often of different magnitude and widely separated in time, but with nearly identical recorded waveforms. Since the details of the recorded waveforms are very sensitive to the source-receiver path and focal mechanism, the high degree of waveform similarity implies that the events originate from virtually the same location and have essentially the same source mechanism. On the basis of analysis of large-scale seismicity in China, *Schaff and Richards* [2004] observed recurrence intervals for most of repeating earthquakes of one month or less, suggesting that most repeating events in China are causally related.

[27] Among the earthquakes in Maniwaki cluster (Figure 10) that we have analyzed from 1980 to 2004, three pairs have remarkably similar waveforms (Figure 12). The events in each pair have almost the same hypocenter, as indicated by the very similar differential time *S-P*, and almost the same focal mechanism, as indicated by the very similar waveform polarities. After band-pass filtering we computed normalized correlation coefficients of more than 0.9 for these three event pairs (Table 5), suggesting that they may be considered as repeating events. Here, the recurrence intervals vary from about 6 months to 6 years. On the basis of *Schaff and Richards'* [2004] interpretation of repeating events, the pairs with repeat interval of 6 months or more may be due to creep loading of stuck fault patches.

8. Possible Relationships of Seismicity to Preexisting Structural Elements

[28] In 1993, 415.5 km of deep crustal vibroseis data were acquired by Canada's LITHOPROBE program along a series of sinuous profiles in western Quebec. This set of seismic profiles transects several major Grenvillian terrane boundaries and runs close to main axis of the WQSZ. The proximity of the seismic profile to the most active part of the WQSZ affords an opportunity to probe the geometric relationships, if any, between the distribution of earthquake hypocenters and Precambrian tectonic structures imaged by the seismic profile.

[29] In order to examine the geological context for WQSZ seismicity, we have projected hypocenters for the events with good depth control into the LITHOPROBE section. Accurate projection of the hypocenters into the seismic section requires a priori knowledge of the geologic strike direction. Figure 13 shows a total intensity magnetic anomaly map, which provides a useful tool to estimate strike information since it highlights the distribution of tectonically controlled geologic units with high magnetic susceptibility. Major Grenvillian tectonic terranes and their bounding structures are clearly delineated by positive and negative magnetic anomaly trends, even in areas where they are covered by (nonmagnetic) Paleozoic cover rocks. The locations of late Precambrian and early Paleozoic faults that

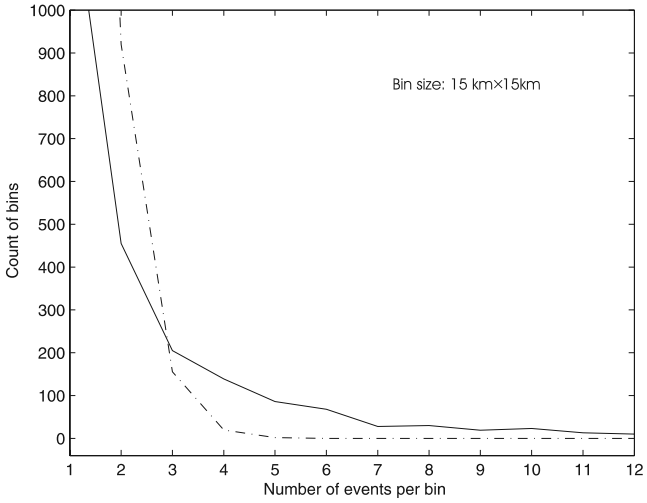

Figure 9. Curves showing the number of events per bin and the corresponding Poisson distribution, using seismicity for the region 42°–49°N and 82°–72°W for the period 1 January 1980 to 1 June 2006 (source Earthquakes Canada online catalog, http://earthquakescanada.nrcan.gc.ca). The solid line was generated with the observed events number; the dashed line was generated with the Poisson distribution formula (equation (4)). Only events with mN $\geq$ 2.0 were used, for which the catalog is effectively complete. Bins with four events and more fall above the Poisson distribution.

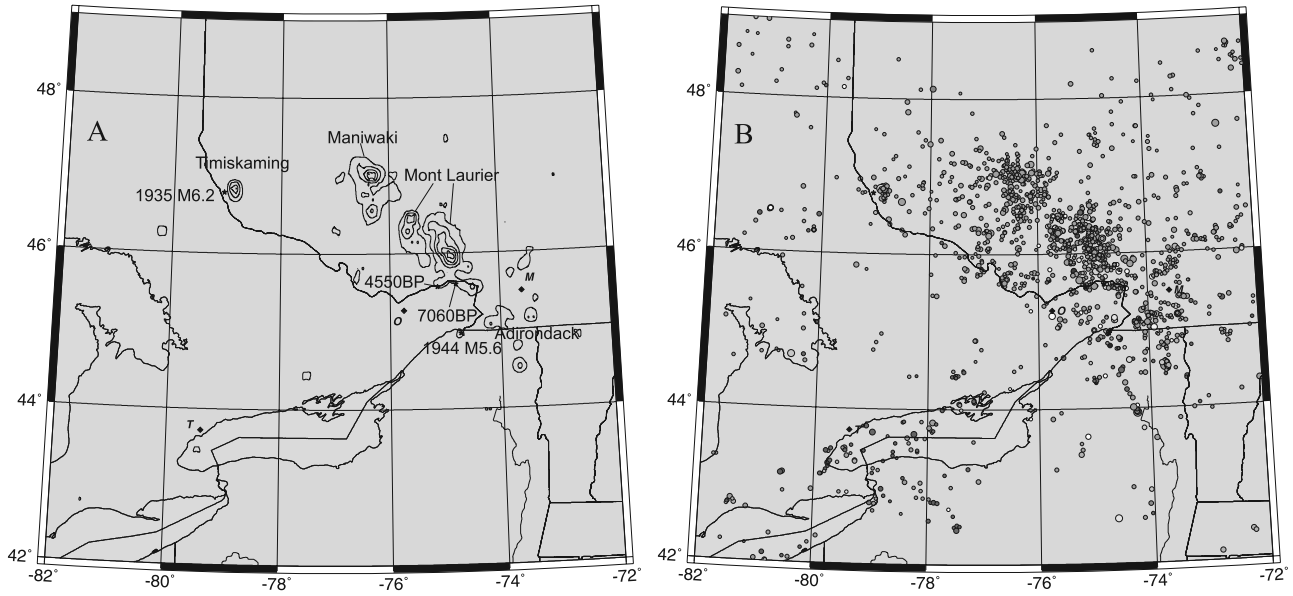

Figure 10. (a) Contour map of the number of events per bin obtained using a bin size of 15 km × 15 km. The lowest contours connect the bins containing four earthquakes; the contour interval is 5 (events per bin). Several clusters are located near historical earthquakes as indicated. (b) Distribution of earthquakes with mN ≥ 2.0 from 1980 to 2006, used in the clustering analysis.

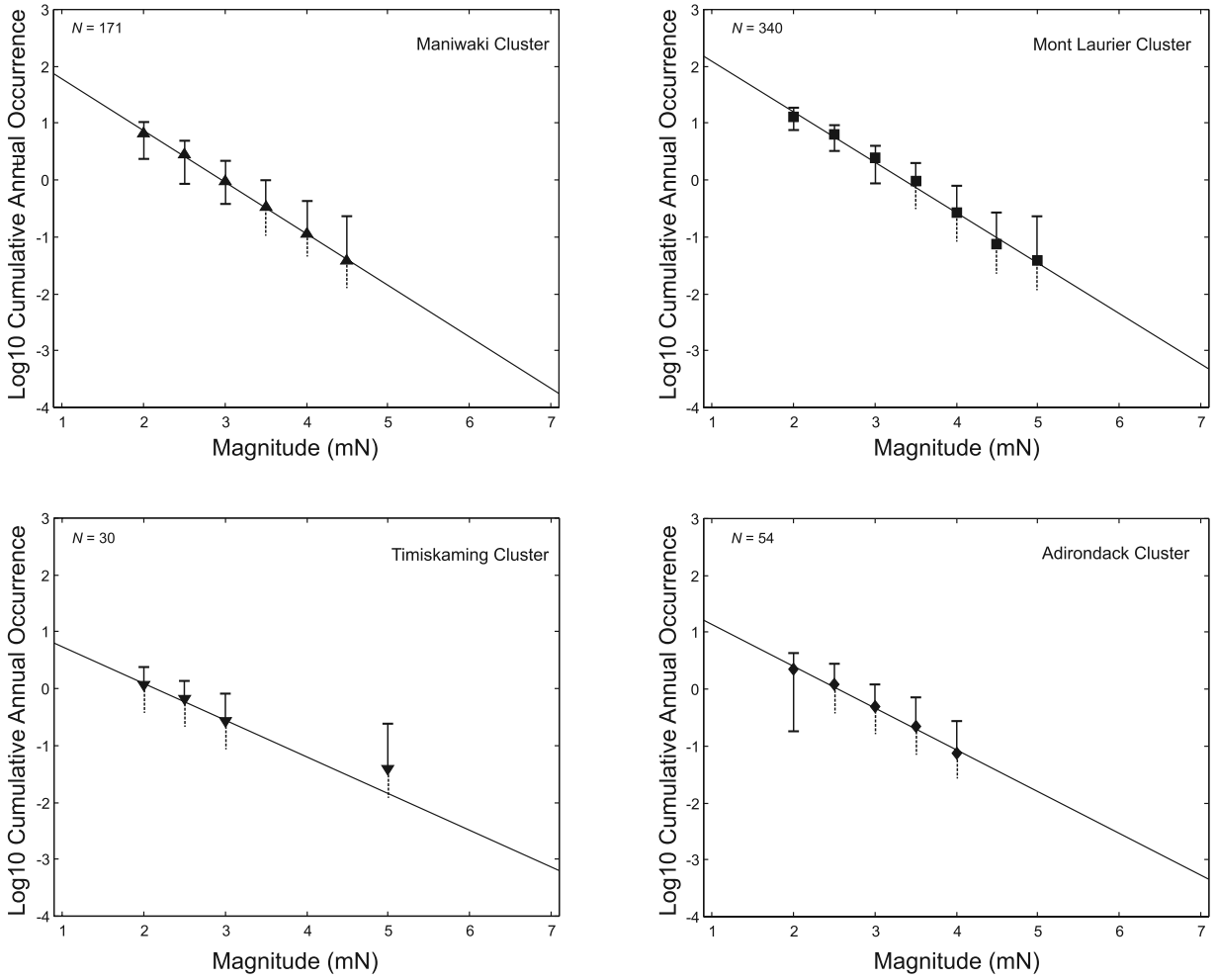

Figure 11. Gutenberg-Richter graphs for individual clusters, showing line of best fit determined by linear regression.

Table 4. Parameters for Seismicity Clusters in the WQSZ

Cluster	Latitude	Longitude	N	*b*	80%[a]	90%[a]	95%[a]	Area, km^2	M[b]	T[c]
Maniwaki	47°	−76.5°	171	0.87	0.08	0.11	0.13	4.8×10^3		
Mont Laurier	46°	−75.5°	340	0.76	0.05	0.07	0.08	9.2×10^3	(>7)	(4500–7600)
Adirondack	45°	−74°	54	0.65	0.10	0.12	0.15	1.9×10^3		
Temiskaming	46.8°	−78.9°	30	0.56	0.15	0.19	0.23	4.9×10^2	6.2	72

[a]Uncertainty in *b* for the indicated confidence level, based on the maximum-likelihood method of *Aki* [1965].
[b]Magnitude of the most recent large (inferred) event near or within the cluster.
[c]Time, in years, since the last large (inferred) event.

bound the Ottawa-Bonnechere graben, as well as the inferred corridor of the Great Meteor hot spot track, are also indicated in Figure 13. These features are not discernible from the magnetic map, but are known from other sources. Open circles on the map indicate epicenters of the 394 depth-located events from combined analysis of *Ma and Atkinson* [2006] and this study.

[30] The LITHOPROBE seismic profile has formed the basis for detailed interpretation of crustal structure in this region [*Martignole and Calvert*, 1996]. A first-order tectonic boundary imaged by the seismic profile (Figure 14) is the Baskatong crustal ramp, which forms an accretionary boundary that separates reworked Archean and Paleoproterozoic rocks of Pre-Grenvillian Laurentia and its margin from allocthonous rocks of the structurally overlying Lac Dumoine and Mont Laurier terranes [*Martignole and Calvert*, 1996]. The rocks in the hanging wall of the Baskatong crustal ramp are interpreted to be disposed in an imbricate series of SE dipping thrust slices that were emplaced during the 1.2–0.98 Ga Grenville orogeny, whereas the footwall zone is composed of reworked parautochtonous rocks, characterized by bands of reflectivity with an apparent NW dip direction. The overall geometry of reflections along the profile defines a major tectonic wedge structure, with clear discordance in the dip of reflectivity beneath and along the crustal ramp.

[31] On the basis of the orientation of the magnetic fabric, estimated to be N45°E for line 52 and N5°E for line 53, we have projected earthquake hypocenters into the plane of the seismic profile (Figure 14). For units above the Baskatong crustal ramp, several linear trends of projected hypocenters are discernible, with an apparent dip toward the SE. One of the trends of projected hypocenters is located close to, but slightly NW of, the interpreted location of the Baskatong crustal ramp. Hypocenters from the Maniwaki cluster that lie beneath this dipping zone do not exhibit any clear preferred direction.

[32] On the basis of previous interpretations of the seismic profile [*Martignole and Calvert*, 1996; *Ludden and Hynes*, 2000]), we interpret the deep seismicity of the Maniwaki cluster to be concentrated within the footwall of the Baskatong crustal ramp, whereas the rest of depth-located WQSZ seismicity is located in the hanging wall. As noted above, there is a slight offset in the position of one of the apparent SE dipping trends of hypocenters with respect to the crustal ramp; however, given uncertainties in projection of the seismicity into the plane of the profile, we believe that this discrepancy does not preclude the

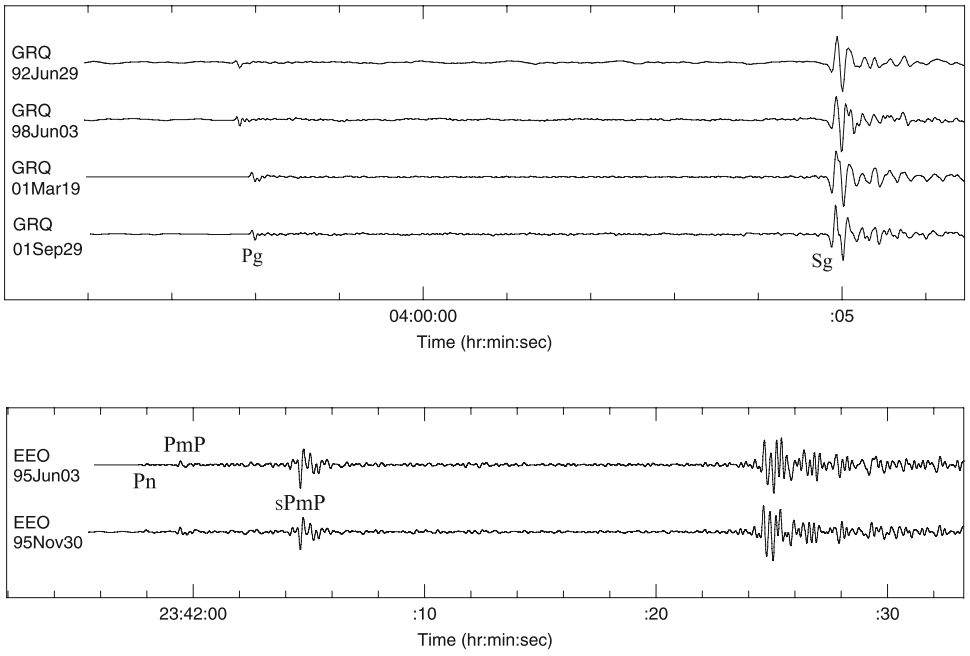

Figure 12. Examples of repeating events from the Maniwaki cluster (Table 5). (top) Waveform comparison at short epicentral distance (∼ 60 km); (bottom) comparison at long epicentral distance (∼ 217 km).

Table 5. Parameters for Inferred Repeating Events in the Maniwaki Cluster

Event	Date	Time, UT	Latitude	Longitude	mN	Correlation Coefficient
1	1992/06/29	1358:51	47.01	−76.34	2.0	0.96[a]
2	1998/06/03	0003:45	47.07	−76.34	2.1	
3	2001/03/19	1040:17	47.05	−76.28	3.9	0.93[a]
4	2001/09/29	1230:14	47.01	−76.24	2.1	
5	1995/06/03	2244:32	47.02	−76.28	3.9	0.90[b]
6	1995/11/30	2341:24	46.99	−76.30	3.1	

[a]Calculated using a 5–10 Hz band-pass filter and a ~9 s time window containing Pg and Sg phases.
[b]Calculated using a 1–6 Hz band-pass filter and a ~9 s time window containing Pn, PmP, and sPmP phases.

possibility that the hypocenters are localized along the structural ramp. Thus the distribution of hypocenters with respect to the major tectonic elements imaged by the crustal seismic profile suggests some evidence for local controls on the distribution of small-scale seismicity by preexisting Precambrian structures.

9. Discussion

[33] Although we observe some evidence that preexisting tectonic fabrics may locally influence the distribution of earthquakes, an overall lack of spatial correlation (Figure 13) appears to falsify the hypotheses that the trend of the WQSZ is primarily controlled by either Mesoproterozoic shear zones associated with the Grenville orogeny [*Forsyth*, 1981] or extensional faults associated with opening of the Iapetus Ocean [*Forsyth*, 1981; *Bent et al.*, 2002; *Adams and Basham*, 1991]. For example, several major Precambrian shear zones in the study region, such as the Baskatong shear zone and the Labelle shear zone, were formed as a result of continent-continent collision and terrane accretion during the 1.2–0.98 Ga Grenville orogeny [*Martignole and Calvert*, 1996; *Ludden and Hynes*, 2000]. These structures generally strike in a NE-SW direction, roughly parallel to the strike of the Grenville Front (Figure 13). Comparison with the distribution of seismicity in the WQSZ shows that the shear zones cut across the NW-SE trend of the WQSZ at a high angle. It seems unlikely that the distribution of seismicity can be explained entirely by reactivation of these structures, or other structures that strike parallel to these shear zones. Indeed, if correct, this hypothesis would be difficult to reconcile with the extent of the Mesoproterozoic shear zones well beyond the vicinity of the WQSZ.

[34] Similarly, with a few exceptions, there is little spatial overlap between clusters of seismicity in the WQSZ and late Precambrian to early Paleozoic extensional faults that bound or obliquely transect the Ottawa-Bonnechere and Timiskaming graben structures (Figure 13). One significant exception is the Timiskaming cluster, which is located within the Timiskaming graben and likely constitutes reverse-sense reactivation of the bounding normal fault at this location [*Bent*, 1996b; *Bent et al.*, 2002]. On the basis of the pattern of seismicity, *Forsyth* [1981] and *Adams and Basham* [1991] proposed that the WQSZ is composed of two narrow subzones. They interpreted events within the western subzone to be controlled (directly or indirectly) by the Ottawa-Bonnechere-Timiskaming graben system, whereas they attributed the eastern subzone to the Great Meteor hot spot track. It is clear, however, that only a small fraction of the overall WQSZ seismicity occurs within the graben systems. In fact, along most of their extents the graben systems are historically aseismic. We therefore prefer a simpler model that encompasses all of the WQSZ seismicity within a single causal framework, rather than invoking different underlying causes of seismicity for inferred neighboring, almost parallel subzones.

[35] As noted above, a remaining hypothesis posits that WQSZ seismicity owes its trend and location to the Great Meteor hot spot track. If this hypothesis is correct, it raises the question of what crustal mechanism actually causes enhanced seismicity along the track. Here, we offer two possible conceptual models. In the first model, the effective age of preexisting faults is thermally reset by the passage of North America over the hot spot (circa 145–130 Ma). In support of this model, we note that a correlation has been established between zones of intraplate seismicity and the locations of Paleozoic and younger normal faults. *Johnston*

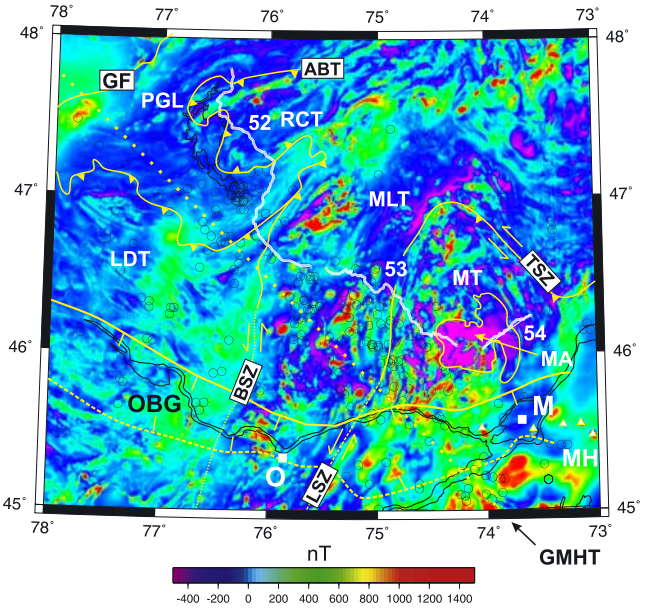

Figure 13. Magnetic anomaly map, along with the locations of the LITHOPROBE seismic profiles 52–54 and seismicity (mN ≥ 2.8). GF denotes Grenville Front; MA denotes Morin Anorthosite; MH denotes Monteregian Hills; MT denotes Morin Terrane, MLT denotes Mont Laurier Terrane; LDT denotes Lac Dumois Terrane; RCT denotes Reservoir Cabonga Terrane; PGL denotes pre-Grenvillian Laurentia; TSZ denotes Taureau shear zone; BSZ denotes Baskatong shear zone; LSZ denotes Labelle shear zone [after *Martignole and Calvert*, 1996]; GMHT denotes the Great Meteor hot spot track.

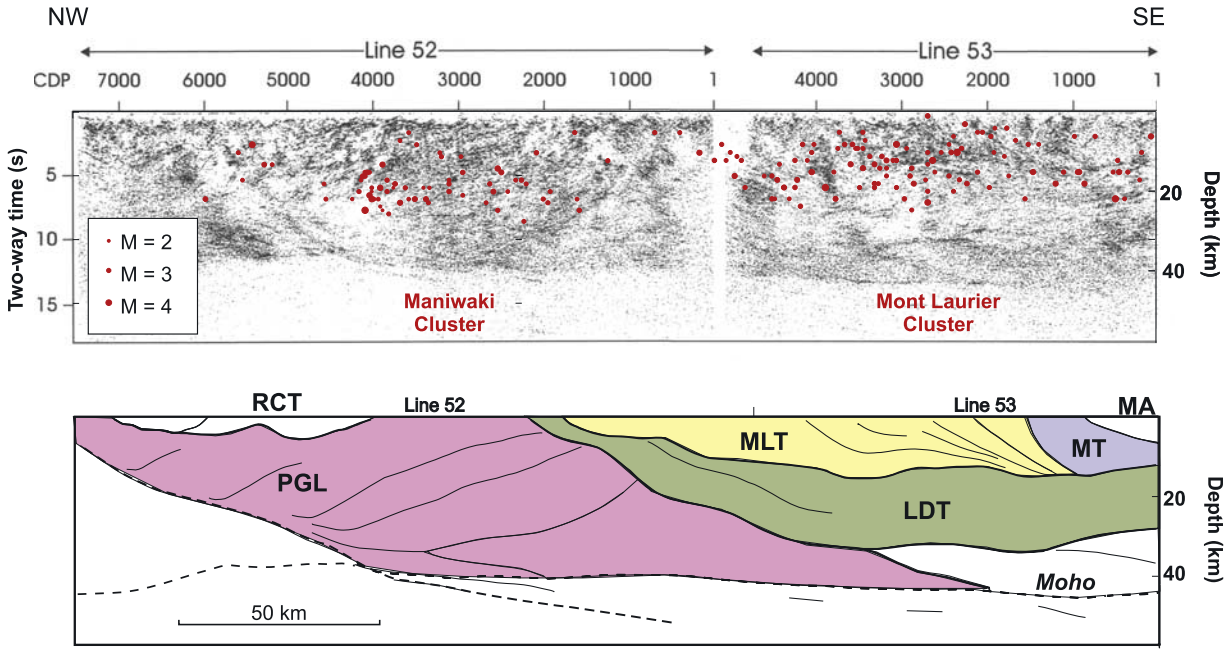

Figure 14. Projection of depth-located earthquake (mN $\geq$ 2.8) hypocenters onto the LITHOPROBE seismic profile through the WQSZ. Abbreviations for geologic units are as in Figure 13. No vertical exaggeration.

and Kanter [1990] and *Johnston et al.* [1994] found that areas that have undergone extension since the Precambrian (such as passive margins and failed rifts) are more likely to experience earthquakes, whereas areas of Precambrian rifting have levels of seismicity similar to stable cratons. Although the faults and shear zones in this area are of Precambrian age, we speculate that reheating, either by thermal diffusion from deep-seated magmatic activity or by advection of heat due to shallower crustal intrusions, could sufficiently weaken these structures to render them mechanically analogous to younger faults. This conceptual model is consistent with the observation that preexisting structures appear to exert a local influence on the seismicity distribution.

[36] A second conceptual model, proposed by *Dineva et al.* [2007], posits that intraplate seismicity may arise from stress concentrations caused by the emplacement of mafic bodies into a more felsic crust [cf. *Gangopadhyay and Talwani*, 2003]. *Dineva et al.* [2007] show that for a cold cratonic geotherm and low strain rates applicable to this region, a strength contrast of more than 8 kbar between plagioclase rich (mafic) and quartz-rich (felsic) rocks peaks at ~17 km depth in the crust. The large strength contrast occurs because thermally activated creep in a felsic lithology tends to occur at much lower temperatures than for a mafic lithology [e.g., *Ranalli*, 1995]. For the WQSZ this model is particularly attractive, since the computed strength contrast between these lithologies is large (>2 kbar) within a depth range of 8–22 km [*Dineva et al.*, 2007], similar to the focal depth distribution of seismicity observed here.

[37] It is also interesting to note that the WQSZ is spatially bracketed by two distinctly different types of inferred hot spot-related magmatism. Toward the interior of Laurentia along the older part of the track, NW of the WQSZ, interpreted hot spot-related magmatism is manifested as small-volume, kimberlite intrusions [*Heaman and Kjaarsgaard*, 2000]. Conversely, toward the plate margin along the younger part of the track, possible hot spot-related magmatism is manifested at the surface as larger-volume plutons within the Monteregian alkaline igneous province [*Eby*, 1984]. If the hot spot model for these magmatic features is correct, it implies that at some location between the kimberlite volcanics NW of the WQSZ and the Monteregian Hills to the SE, mantle-derived melts breached the lithosphere, allowing passage of significant volumes of magma to the surface. Here, we propose that the WQSZ represents an intervening region of blind intrusions associated with the hot spot. Possible entrapment of mantle-derived melts within the crust, implied by this interpretation, is consistent with both of the conceptual models described above. Entrapment of mantle-derived melt in the crust would provide a local heat source that could rejuvenate older fault zones, or alternatively could represent a mechanism for emplacement of mafic bodies that may serve as stress concentrators in the middle crust. We remark that the hypothesis that the WQSZ is underlain by blind midcrustal mafic intrusions is testable by modeling and inversion of gravity data, since it is expected that the relatively high density of mafic rocks intruded into a more felsic crust should have a gravity signature. A test of this hypothesis is currently underway.

[38] It has been suggested that present-day seismicity in eastern North America could be strongly influenced by crustal stress perturbations caused by postglacial isostatic adjustment (PIA) [e.g., *Adams*, 1989; *Zoback*, 1992; *James and Bent*, 1994; *Wu*, 1998; *Mazzotti et al.*, 2005]. Both tectonic stresses and PIA appear to be necessary to explain the nature and distribution of seismicity in formerly glaci-

ated terranes of eastern Canada [*Stewart et al.*, 2000]. At a regional scale, seismicity of the WQSZ is undoubtedly influenced by PIA, but PIA cannot entirely explain the localization of seismicity along the observed linear trend.

[39] Finally, the results of our clustering analysis provide significant evidence for spatial clustering of microseismicity coincident with or near the locations of large historic and prehistoric events. It is worth noting that characteristics of the Timiskaming cluster, close to the epicenter of the 1935 *M*6.2 earthquake, differs in several important respects from characteristics of other seismicity clusters (Mont Laurier, Adirondack) that are located near two inferred prehistoric events NE of Ottawa. First, the Timiskaming cluster has a smaller area than the other large clusters, consistent with the notion that seismicity clusters reflect the rupture area of past earthquakes. If the prehistoric earthquakes near Ottawa were of magnitude 7 or greater, as suggested by *Aylesworth et al.* [2000], then the rupture dimension would also be greater than at Timiskaming. Secondly, the Timiskaming cluster is characterized by a lower Gutenberg-Richter *b* value than the other clusters. For example, the difference in *b* value with respect to the Maniwaki cluster is significant at the 90% confidence level (Table 4). Our results are thus qualitatively consistent with a slow reduction, on a timescale of thousands of years, in *b* value with time since the last major rupture [*Ebel et al.*, 2000].

10. Conclusions

[40] The western Quebec seismic zone (WQSZ), the main source of earthquake hazard for the cities of Ottawa and Montreal [*Adams and Halchuk*, 2003], is composed of a series of earthquake clusters that collectively form a NW trending elongate band of intraplate seismicity measuring $\sim$ 160 km wide and 500 km long. In this study, spatial clusters of seismicity within the WQSZ are identified using a novel statistical technique that highlights regions where the seismicity rate exceeds the level for a purely random earthquake distribution based on a Poisson model. The most intensively studied cluster (Maniwaki) shows evidence for repeating earthquakes with repeat times of more than 6 months, suggestive of creep loading of stuck fault patches [*Schaff and Richards*,]. Using a regional depth phase modeling technique, we show that the seismicity within the WQSZ occurs at greater focal depth (5–26 km) than surrounding background seismicity (2–6 km). Focal mechanisms of events, including a new focal mechanism for a moderate earthquake on 25 February 2006 near Buckingham, Québec, reveal a broadly consistent pattern of NE-SW *P* axes although variations in focal mechanism exist throughout the region [*Kim et al.*, 2006]. On the basis of projection of depth-located hypocenters onto a high-quality LITHOPROBE seismic profile, we find that the distribution of earthquakes in the WQSZ may be locally influenced by Precambrian structures associated with the Grenville orogeny and rifting associated with opening of the Iapetus Ocean. The primary factor controlling the location of the WQSZ, however, is the Mesozoic track of the Great Meteor hot spot. We propose that the hot spot track exerts control on the location of seismicity, either by thermal rejuvenation of antecedent faults, or by stress concentration due to a predicted large strength contrast between mafic and felsic rock in the middle crust [*Dineva et al.*, 2007]. The locations and characteristics of seismicity clusters appear to be consistent with the hypothesis that they represent exceptionally persistent aftershocks of past large earthquakes [*Ebel et al.*, 2000; *Ma and Atkinson*, 2006].

[41] **Acknowledgments.** This work was funded by the Natural Sciences and Engineering Research Council of Canada (NSERC) and by the Ontario Rand Challenge fund. We gratefully acknowledge the constructive review comments and suggestions from Associate Editor Joan Gomberg and the two anonymous reviewers.

References

Adams, J. (1989), Postglacial faulting in eastern Canada: Nature, origin and seismic hazard implications, *Tectonophysics*, *163*, 323–331.

Adams, J., and P. Basham (1989), The seismicity and seismotectonics of Canada east of the Cordillera, *Geosci. Can.*, *16*(1), 3–16.

Adams, J., and P. Basham (1991), The seismicity and seismotectonics of eastern Canada, in *Neotectonics of North America*, edited by D. B. Slemmons et al., pp. 261–276, Geol. Soc. of Am., Boulder, Colo.

Adams, J., and S. Halchuk (2003), Fourth generation seismic hazards maps for Canada: Values for over 650 Canadian localities intended for the 2005 National Building Code of Canada, *Open File 4459*, 155 pp., Geol. Surv. of Can., Ottawa, Ont.

Aki, K. (1965), Maximum likelihood estimate of b in the formula logN = a-bM and its confidence limits, *Bull. Earthquake Res. Inst.*, *43*, 237–239.

Atkinson, G., and E. Sonley (2003), Ground motions from the 2002 Au Sable Forks New York M5.0 earthquake, *Seismol. Res. Lett.*, *74*, 339–349.

Aylsworth, J. M., D. E. Lawrence, and J. Guertin (2000), Did two massive earthquakes in the Holocene induce widespread landsliding and near-surface deformation in part of the Ottawa Valley, Canada?, *Geology*, *28*, 903–906.

Basham, D. M., D. H. Weichert, and M. J. Berry (1979), Regional assessment of seismic risk in eastern Canada, *Bull. Seismol. Soc. Am.*, *11*, 1567–1602.

Bent, A. L. (1996a), Source parameters of the damaging Cornwall-Massena earthquake of 1944 from regional waveforms, *Bull. Seismol. Soc. Am.*, *86*, 489–497.

Bent, A. L. (1996b), An improved source mechanism for the 1 935 Timiskaming, Quebec earthquake from regional waveforms, *Pure Appl. Geophys.*, *146*, 5–20.

Bent, A. L., M. Lamontagne, J. Adams, C. R. D. Woodgold, S. Halchuk, J. Drysdale, R. J. Wetmiller, S. Ma, and J.-B. Dastous (2002), The Kipawa, Quebec "Millennium" earthquake, *Seismol. Res. Lett.*, *73*, 285–297.

Buchbinder, G. G. R., A. Lambert, R. D. Kurtz, D. R. Bower, F. M. Anglin, and J. Peters (1988), Twelve years of geophysical research in the Charlevoix seismic zone, *Tectonophysics*, *156*, 193–224.

Carr, S. D., R. M. Easton, R. A. Jamieson, and N. G. Culshaw (2000), Geologic transect across the Grenville orogen of Ontario and New York, *Can. J. Earth Sci.*, *27*, 193–216.

Crough, S. T. (1981), Mesozoic hotspot epeirogeny in eastern North America, *Geology*, *9*, 2–6.

Dineva, S., D. Eaton, S. Ma, and R. Mereu (2007), The October 2005 Georgian Bay (Canada) earthquake sequence: Mafic dykes and their role in the mechanical heterogeneity of Precambrian crust, *Bull. Seismol. Soc. Am.*, *97*(2), 457–473, doi:10.1785/0120060176.

Doig, R. (1991), Effects of strong seismic shaking in lake sediments, and earthquake recurrence interval, Timiscaming, Quebec, *Can. J. Earth Sci.*, *28*, 1349–1352.

Du, W.-X., W.-Y. Kim, and L. R. Sykes (2003), Earthquake source parameters and state of stress for the northeastern United States and southeastern Canada from analysis of regional seismograms, *Bull. Seismol. Soc. Am.*, *93*, 1633–1648.

Eaton, D., et al. (2005), Investigating Canada's lithosphere and earthquake hazards with portable arrays, *Eos Trans. AGU*, *86*(17), 169, 173.

Eaton, D., S. Dineva, and R. Mereu (2006), Crustal thickness and Vp/Vs variations in the central Grenville orogen (Ontario, Canada) from analysis of teleseismic receiver functions, *Tectonophysics*, *420*, 223–238.

Ebel, J. E. (1998), Speculations on the source parameters of the 1638 earthquake in the northeastern United States using inferences from modern seismicity, paper presented at the 70th Annual Meeting, East. Sect. Seismol. Soc. of Am., Millersville, Pa., 18–20 Oct.

Ebel, J. E. (2000), A reanalysis of the 1727 earthquake at Newbury Massachusetts, *Seismol. Res. Lett.*, *71*(3), 364–374.

Ebel, J. E. (2002), A new look at the 1755 Cape Ann Massachusetts earthquake, *Seismol. Res. Lett.*, *73*, 418–419.

Ebel, J. E., K. P. Bonjer, and M. C. Oncescu (2000), Paleoseismicity: Seismicity evidence for past large earthquakes, *Seismol. Res. Lett.*, *71*, 283–294.

Eby, G. N. (1984), Geochronology of the Monteregian Hills alkaline igneous province Quebec, *Geology*, *12*, 468–470.

Faill, R. T. (1997), A geologic history of the north-central Appalachians: part 1. Orogenesis from the Mesoproterozoic through the Taconic orogeny, *Am. J. Sci.*, *297*, 551–619.

Forsyth, D. A. (1981), Characteristics of the western Quebec seismic zone, *Can. J. Earth Sci.*, *18*, 103–119.

Gangopdhyay, A., and P. Talwani (2003), Symptomatic features of intraplate earthquakes, *Seismol. Res. Lett.*, *74*, 863–883.

Haddon, R. A. W. (1995), Modelling of source rupture characteristics for the Saguenay earthquake of November 1988, *Bull. Seismol. Soc. Am.*, *85*, 525–551.

Heaman, L. M., and B. A. Kjarsgaard (2000), Timing of eastern North American kimberlite magmatism: Continental extension of the Great Meteor hotspot track?, *Earth Planet. Sci. Lett.*, *178*, 253–268.

Herrmann, R. B. (1978), A seismological study of two Attica New York earthquakes, *Bull. Seismol. Soc. Am.*, *68*, 641–651.

Herrmann, R. B. (2002), Computer programs in seismology, Dep. of Earth and Atmos. Sci., Saint Louis Univ., Saint Louis, Mo.

Hodgson, E. A. (1936a), Preliminary report of the earthquake of November 1, 1935, *Earthquake Notes*, *7*(4), 1–4.

Hodgson, E. A. (1936b), The Timiskaming earthquake of November 1st, 1935: The location of epicenter and determination of focal depth, *J. R. Astron. Soc. Can.*, *30*(4), 113–123.

Hodgson, E. A. (1945), The Cornwall-Massena earthquake, September 5, 1944, *J. R. Astron. Soc. Can.*, *39*(1), 5–13.

Horner, R. B., A. E. Stevens, H. S. Hasegawa, and G. Leblanc (1978), Focal parameters of the July 12, 1975, Maniwaki, Québec, earthquake—An example of intraplate seismicity in eastern Canada, *Bull. Seismol. Soc. Am.*, *68*, 619–640.

James, T. S., and A. L. Bent (1994), A comparison of eastern North American seismic strain rates to glacial rebound strain-rates, *Geophys. Res. Lett.*, *21*, 2127–2130.

Johnston, A. C., and L. R. Kanter (1990), Earthquakes in stable continental crust, *Sci. Am.*, *262*(3), 68–75.

Johnston, A. C., K. J. Coppersmith, L. R. Kanter, and C. A. Cornell (1994), The earthquakes of stable continental regions, vol. 1, Assessment of large earthquake potential, *Tech. Rep. TR-102261-VI*, Electr. Power Res. Inst., Palo Alto, Calif.

Kamo, S. L., T. E. Krogh, and P. S. Kumarapeli (1995), Age of the Grenville dyke swarm, Ontario Quebec: Implications for the timing of Iapetan rifting, *Can. J. Earth Sci.*, *32*, 273–280.

Kim, W.-Y., S. Dineva, S. Ma, and D. Eaton (2006), The 4 August 2004 Lake Ontario, earthquake, *Seismol. Res. Lett.*, *77*, 65–73.

Lamontagne, M., H. S. Hasegawa, D. A. Forsyth, G. G. R. Buchbinder, and M. Cajka (1994), The Mont-Laurier, Québec, earthquake of 19 October 1990 and its seismotectonic environment, *Bull. Seismol. Soc. Am.*, *84*, 1505–1522.

Leblanc, G. (1981), A closer look at the September 16, 1732 Montreal earthquake, *Can. J. Earth Sci.*, *18*, 539–550.

Ludden, J., and A. Hynes (2000), The LITHOPROBE Abitibi-Grenville transect: Two billion years of crust formation and recycling in the Precambrian Shield of Canada, *Can. J. Earth Sci.*, *37*, 459–476.

Ma, S., and J. Adams (2002), Estimation of moment tensor for moderate earthquakes in eastern Canada and its vicinity by modeling surface waveforms, internal report, 110 pp., Nat. Resour. Can., Ottawa.

Ma, S., and G. M. Atkinson (2006), Focal depth distribution for earthquakes with $mN \geq 2.8$ in western Quebec, southern Ontario, and northern New York, *Bull. Seismol. Soc. Am.*, *96*, 609–623.

Ma, S., V. Peci, J. Adams, and D. McCormack (2003), Routine estimate of focal depths for moderate and small earthquakes by modeling regional depth phase sPmP in eastern Canada, *Geophys. Res. Abstr.*, *5*, Abstract 6176.

Martignole, J., and A. J. Calvert (1996), Crustal-scale shortening and extension across the Grenville province of western Quebec, *Tectonics*, *15*, 376–386.

Mazzotti, S., T. S. James, J. Henton, and J. Adams (2005), GPS crustal strain, postglacial rebound, and seismic hazard in eastern North America: The Saint Lawrence valley example, *J. Geophys. Res.*, *110*, B11301, doi:10.1029/2004JB003590.

McHone, J. G. (1996), Constraints on the mantle plume model for Mesozoic alkaline intrusions in northeastern North America, *Can. Mineral.*, *43*, 325–334.

Mereu, R. F., et al. (1986), The 1982 COCRUST seismic experiment across the Ottawa-Bonnechere graben and Grenville front in Ontario and Québec, *Geophys. J.R. Astron. Soc.*, *84*, 491–514.

Morgan, W. J. (1983), Hotspot tracks and the early rifting of the Atlantic, *Tectonophysics*, *94*, 123–139.

Nabelek, J., and G. Suarez (1989), The 1983 Goodnow earthquake in the central Adirondacks, N.Y.: Rupture of a simple circular crack, *Bull. Seismol. Soc. Am.*, *79*, 1762–1777.

Nuttli, O. W. (1973), Seismic wave attenuation and magnitude relations for eastern North America, *J. Geophys. Res.*, *78*, 876–885.

Pierre, J. R., and M. Lamontagne (2004), The 20 April 2002, M_w5.0 Au Sable Forks, New York, earthquake: A supplementary source of knowledge on earthquake damage to lifelines and buildings in eastern North America, *Seismol. Res. Lett.*, *75*, 626–636.

Prigmore, J. K., A. J. Butler, and N. H. Woodcock (1997), Rifting during separation of eastern Avalonia from Gondwana: Evidence from subsidence analysis, *Geology*, *25*, 203–206.

Ranalli, G. (1995), *Rheology of the Earth*, 2nd ed., Chapman and Hall, London.

Randall, G. (1994), Efficient calculation of complete differential seismograms for laterally homogeneous Earth models, *Geophys. J. Int.*, *118*, 245–254.

Rivers, T. (1997), Lithotectonic elements of the Grenville Province: Review and tectonic implications, *Precambrian Res.*, *86*, 117–154.

Saikia, C. K. (1992), Numerical study of quarry generated Rg as a discriminant for earthquakes and explosions: Modeling of Rg in southwestern New England, *J. Geophys. Res.*, *97*, 11,057–11,072.

Schaff, D. P., and P. Richards (2004), Repeating seismic events in China, *Science*, *303*, 1176–1178.

Seeber, L., W.-Y. Kim, J. Armbruster, W.-X. Du, and A. Lerner-Lam (2002), The 20 April 2002 M_w5.0 earthquake near Au Sable Forks, Adirondacks, New York: A first glance at a new sequence, *Seismol. Res. Lett.*, *73*, 480–489.

Sleep, N. H. (1990), Monteregian hotspot track: A long-lived mantle plume, *J. Geophys. Res.*, *95*, 21,983–21,990.

Smith, W. E. T. (1962), Earthquakes of eastern Canada and adjacent areas 1534–1927, *Publ. Dominion Obs. Ottawa*, *26*, 269–301.

Stein, S., and M. Wysession (2003), *An Introduction to Seismology, Earthquakes, and Earth Structure*, Blackwell, Malden, Mass.

Stewart, I. S., J. Sauber, and J. Rose (2000), Glacio-tectonics: Ice sheets, crustal Deformation, and seismicity, *Quat. Sci. Rev.*, *19*, 1367–1389.

Swan, A. R. H., and M. Sandilands (1995), *Introduction to Geological Data Analysis*, Blackwell Sci., Malden, Mass.

Sykes, L. R. (1980), Earthquakes and other processes within lithospheric plates and the reactivation of pre-existing zones of weakness, in *The Continental Crust and Its Mineral Deposits*, edited by D. W. Strangway, *Geol. Assoc. Can. Spec. Pap.*, *20*, 215–237.

Wessel, P., and W. H. F. Smith (1998), New, improved version of the Generic Mapping Tools released, *Eos Trans. AGU*, *79*(47), 579.

Wu, P. (1998), Intraplate earthquakes and postglacial rebound in eastern Canada and northern Europe, in *Dynamics of the Ice Age Earth: A Modern Perspective*, edited by P. Wu, pp. 603–628, Trans Tech, Zurich, Switzerland.

Zartman, R. E. (1977), Geochronology of some alkaline rock provinces in eastern and central United States, *Annu. Rev. Earth Planet. Sci.*, *5*, 257–286.

Zoback, M. L. (1992), Stress field constraints on intraplate seismicity in eastern North America, *J. Geophys. Res.*, *97*, 11,761–11,782.

D. W. Eaton and S. Ma, Department of Earth Sciences, University of Western Ontario, 1151 Richmond Street, London, ON, Canada N6A 5B7. (sma44@uwo.ca)